The N-Terminal A Domain of *Staphylococcus aureus* Fibronectin-Binding Protein A Binds to Tropoelastin†

Fiona M. Keane,‡ Adam W. Clarke,§ Timothy J. Foster,‡ and Anthony S. Weiss*,§

Department of Microbiology, Moyne Institute of Preventive Medicine, Trinity College, Dublin 2, Ireland, and School of Molecular and Microbial Biosciences, University of Sydney, Sydney, New South Wales 2006, Australia

Received October 2, 2006; Revised Manuscript Received April 9, 2007

ABSTRACT: *Staphylococcus aureus* is an important human pathogen. Its virulence factors include a variety of MSCRAMMs (microbial surface component recognizing adhesive matrix molecules), each capable of binding specifically to the host extracellular matrix. The fibronectin-binding protein, FnBPA, has been shown previously to bind immobilized fibronectin, fibrinogen, and α-elastin peptides. Here we show that region A of FnBPA (rAFnBPA) binds to recombinant human tropoelastin. Binding occurs to three separate truncates of tropoelastin, encompassing domains 2−18, 17−27, and 27−36, signifying that the interaction occurs at multiple sites. The greatest affinity was for the N-terminal truncate. We observed a pH dependency for the rAFnBPA−tropoelastin interaction with strong, nonsaturable binding at low pH. The interaction ceased at higher pH. These data support a model of surface−surface interactions between the negative charges present on rAFnBPA and the positive lysines of tropoelastin. A protein lacking the negatively charged C-terminal fibronectin-binding motif of the A domain of FnBPA and another construct lacking subdomain N1 were both capable of binding immobilized tropoelastin with a lower affinity. The binding properties of five site-directed mutants of rAFnBPA were compared with wild-type rAFnBPA. There was no decreased affinity for immobilized tropoelastin, in contrast to the defective binding of these mutants to α-elastin and fibrinogen. The data indicate novel interactions between tropoelastin and FnBPA that include the use of surface charges. These results demonstrate that FnBPA is capable of directly binding tropoelastin prior to its incorporation into elastin.

Staphylococcus aureus is a commensal organism of the human anterior nares and skin (*1*). It is also an important opportunistic pathogen. It is the most common cause of hospital-acquired infection and can give rise to a wide variety of diseases ranging from superficial skin infections such as boils and abscesses to more invasive, life-threatening conditions such as pneumonia, septicemia, and infective endocarditis (*2*). Such infections depend on the ability of the bacterium to adhere to and interfere with the host's extracellular matrix (ECM).[1] *S. aureus* possesses several surface-exposed ligand-binding MSCRAMMs (microbial surface component recognizing adhesive matrix molecules) that mediate attachment to host ECM proteins such as fibrinogen (*3*−*5*), fibronectin (*6*, *7*), collagen (*8*), and keratin (*9*). The initial adherence and colonization process is a vital step in the pathogenesis of *S. aureus* infections as indicated by loss of virulence of mutants in infection models. MSCRAMMs typically contain an N-terminal secretory signal sequence, followed by a ligand-binding A domain, other repeated domains, and a cell wall anchoring motif.

The focus of this paper is the fibronectin-binding MSCRAMM, FnBPA (Figure 1). The protein is named after the function first ascribed to it, which is its fibronectin-binding ability. This is now known to be conferred by the 11 tandem repeats recently located between the N-terminal A domain and the wall spanning and anchoring domains (*10*, *11*). The A domain is divided into three subdomains termed N1, N2, and N3 and is responsible for the binding of FnBPA to fibrinogen and elastin (*5*, *12*). While the function of N1 remains unknown, the N2 and N3 subdomains are crucial for ligand binding (*13*). They are homologous to the equivalent domains of clumping factor A, another MSCRAMM of *S. aureus*, and indeed bind the same region of the γ chain of fibrinogen (*5*). On the basis of functional and sequence similarity, N2 and N3 have been predicted to adopt a folded structure similar to that of ClfA (*14*). A 3-D structural model of the N2 and N3 subdomains of FnBPA was previously constructed on the basis of the known crystal structure of ClfA (*13*). In addition, a peptide comprising the C-terminal eight residues of the γ chain of fibrinogen (G_{404}AKQAGDV_{411}) was docked in silico into the putative ligand-binding trench between domains N2 and N3 (Figure 2). This aided in the prediction of residues that may be important for ligand binding. Alanine substitution of residues N304, F306, and R224 caused a significant decrease in the affinity of recombinant A domain proteins for immobilized fibrinogen

† A.S.W. received funding from the Australian Research Council and the University of Sydney. T.J.F. received funding from the Health Research Board of Ireland.

* To whom correspondence should be addressed. Tel: +61 2 9351 3464. Fax: +61 2 9351 4726. E-mail: a.weiss@mmb.usyd.edu.au.

‡ Trinity College.

§ University of Sydney.

[1] Abbreviations: FnBPA, fibronectin-binding protein A; MSCRAMM, microbial surface component recognizing adhesive matrix molecules; ECM, extracellular matrix; ClfA, clumping factor A; SPR, surface plasmon resonance; RU, response units; k_a, association rate; k_d, dissociation rate; K_D, equilibrium dissociation constant.

10.1021/bi700454x CCC: $37.00
Published on Web 05/22/2007

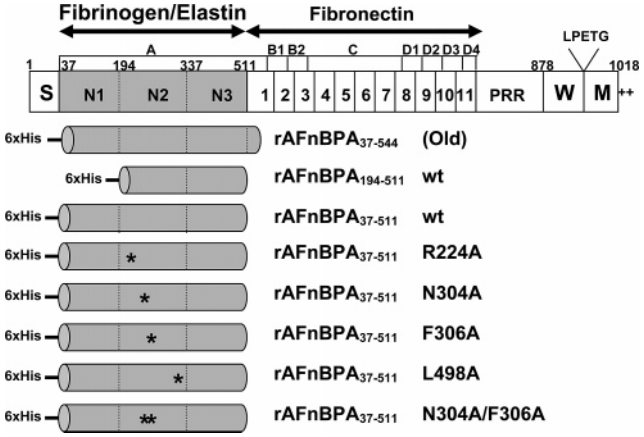

FIGURE 1: Structural organization of the fibronectin-binding protein, FnBPA, of *S. aureus* and recombinant truncated derivatives. A secretory signal sequence (S), region A (gray, divided into subdomains N1, N2, and N3), regions B, C, and D (divided into fibronectin-binding tandem repeats 1−11), cell wall and membrane-anchoring domains (W, M), and modified regions (*) are indicated. This surface-expressed protein is multifunctional, capable of binding immobilized fibronectin via the 11 C-terminal repeated motifs while the A domain functions in adhering to immobilized fibrinogen and elastin peptides.

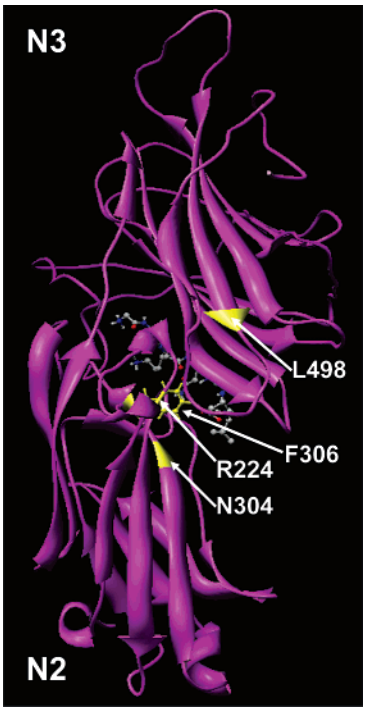

FIGURE 2: 3-D structural model of rAFnBPA. Predicted 3-D structure of $rAFnBPA_{194-511}$ (N23) with the 8-mer fibrinogen ligand (shown in ball and stick format) docked into the trench between N2 and N3 of this structure. Amino acids R224, N304, F306, and L498 of FnBPA are shown in yellow with the side chain of F306 visible in ball and stick format. The side chains of these four residues point into the ligand-occupied space and are involved in ligand binding.

and elastin. The N304A/F306A double substitution was completely defective in ligand binding (*13*).

Elastin is a polymeric protein that provides resilience and elasticity to skin, blood vessels, lungs, ligaments, and tendons. The elastin precursor, tropoelastin, which is composed of alternating hydrophobic and hydrophilic domains, is secreted during fetal development by smooth muscle cells, endothelial cells, and fibroblasts (*15*). The thermodynamically controlled process of coacervation concentrates and aligns tropoelastin monomers into an ordered fibrillar structure on the surface of the cell (*16*) whereby lysine residues in the hydrophilic domains are rapidly cross-linked both intermolecularly and intramolecularly by the enzyme lysyl oxidase to form mature elastin. Commercial elastin peptides, which were used in earlier FnBPA binding assays, are solubilized by boiling elastin-rich tissue in oxalic acid. The resulting soluble elastin peptides, termed α-elastin, are heterogeneous in nature and contain no intact tropoelastin molecules.

We hypothesize that *S. aureus* is capable of compounding its pathogenicity by interacting with secreted tropoelastin and inhibiting de novo elastogenesis because infecting cells are proximal to elastogenic cell surfaces. An important aspect in understanding the *S. aureus*−elastin interaction is to assess if the bacterium is capable of binding tropoelastin. Tropoelastin is composed of alternating hydrophobic and hydrophilic domains with the hydrophilic domains containing lysine residues that are involved in cross-linking. Hydrophobic domains consist primarily of the four amino acids, glycine, alanine, valine, and proline, which constitute 75% of the protein. This recombinant tropoelastin construct has been used extensively to study the interactions with multiple host proteins including fibrillin-1 (*17*), microfibril-associated glycoprotein 1 (MAGP-1) (*18*), and integrin $\alpha_V\beta_3$ (*19*).

The aims of this study were to assess the ability of recombinant FnBPA A domain to bind immobilized tropoelastin and to investigate this interaction using truncated tropoelastin fragments, five alanine-substituted variants of rAFnBPA, and truncated recombinant FnBPA.

MATERIALS AND METHODS

Reagents. Recombinant human tropoelastin (full length, SHELN-18, SHEL17−27, and SHEL27-C) was prepared as described previously (*19*). $rAFnBPA_{37-544}$, $rAFnBPA_{194-511}$, $rAFnBPA_{37-511}$ wt, $rAFnBPA_{37-511}$ R224A, $rAFnBPA_{37-511}$ N304A, $rAFnBPA_{37-511}$ F306A, $rAFnBPA_{37-511}$ L498A, and $rAFnBPA_{37-511}$ N304A/F306A were constructed as described previously (*13*) and purified by nickel affinity chromatography from *Escherichia coli* Topp3 cells bearing the expression vector pQE30. The purity of each construct was examined using SDS−PAGE, and the concentration was determined using the BCA protein assay (Pierce).

Surface Plasmon Resonance Analysis of Molecular Interactions. Kinetic analysis of the binding between tropoelastin and rAFnBPA proteins was performed using surface plasmon resonance (SPR) on a Biacore 3000 system (Biacore AB, Sweden). Full-length human tropoelastin, SHELN-18, SHEL17−27, and SHEL27-C were immobilized onto the surface of a CM5 research-grade sensor chip using amine coupling. This was performed using 1-ethyl-3-(3-dimethylaminopropyl)carbodiimide hydrochloride (EDC), followed by *N*-hydroxysuccinimide (NHS) and ethanolamine hydrochloride, as described by the manufacturer. Tropoelastin proteins were dissolved in 10 mM sodium acetate at pH 5.0 and then immobilized on the chip at a flow rate of 30 μL/min in HBS−Ca buffer (10 mM HEPES, pH 7.2, 0.2 M NaCl, 1 mM $CaCl_2$, 0.005% Tween 20). This gave the following response levels: tropoelastin = 4500 RU, SHELN-18 = 750 RU, SHEL17−27 = 3000 RU, and SHEL27-C =

850 RU. On a single flow cell, the dextran matrix was treated as described above but without tropoelastin present to provide a blank flow cell for these studies. All sensorgram data presented were subtracted from the corresponding data from the blank cell. The response generated from injection of buffer over the chip was also subtracted from all sensorgrams. The data were normalized to aid in comparing sensorgrams from different tropoelastin constructs.

rAFnBPA$_{37-544}$ Binding to Tropoelastin Using SPR. Sensorgrams were obtained for rAFnBPA$_{37-544}$ binding to immobilized tropoelastin using HBS−Ca buffer. rAFnBPA$_{37-544}$ was prepared by doubling dilutions in HBS−Ca to concentrations starting at 500 nM. These concentrations were injected for 8.33 min at a flow rate of 30 μL/min with a sampling rate of 5 Hz. Regeneration was performed after 60 min of dissociation using 1 M NaCl and 10 mM glycine for 2 min. A typical experiment used 10 rAFnBPA protein concentrations and a control containing no rAFnBPA, followed by a regeneration step that was measured successful when the baseline returned to zero.

rAFnBPA$_{37-544}$ Binding to Tropoelastin Constructs Using SPR. Sensorgrams were obtained for rAFnBPA$_{37-544}$ binding to immobilized tropoelastin constructs using HBS−Ca buffer. rAFnBPA$_{37-544}$ at various concentrations (1 μM−3.9 nM for immobilized SHELN-18, 1 μM−3.1 nM for immobilized SHEL17−27, and 2 μM−1.9 nM for immobilized SHEL27-C) was prepared by doubling dilutions in HBS along with a control containing no rAFnBPA$_{37-544}$. These concentrations were injected for 8.33 min at a flow rate of 30 μL/min with a sampling rate of 5 Hz. Regeneration was performed after 60 min of dissociation using 1 M NaCl and 10 mM glycine for 2 min. All experiments were performed in duplicate.

rAFnBPA$_{194-511}$, rAFnBPA$_{37-511}$ wt, and rAFnBPA$_{37-511}$ Site-Directed Mutants Binding to Tropoelastin Using SPR. Sensorgrams were obtained for rAFnBPA proteins binding to immobilized tropoelastin using HBS−Ca buffer. rAFnBPA$_{194-511}$, rAFnBPA$_{37-511}$ wt, and rAFnBPA$_{37-511}$ site-directed mutants were prepared by doubling dilutions in HBS−Ca to concentrations starting at 800 nM. These concentrations were injected for 8.33 min at a flow rate of 30 μL/min. Regeneration was performed after 30 min of dissociation using 1 M NaCl, 0.05 M NaOH, and 10 mM glycine for 2 min. A typical experiment used 10 rAFnBPA protein concentrations and a control containing no rAFnBPA, followed by a regeneration step that was measured successful when the baseline returned to zero.

Effect of pH on rAFnBPA$_{37-544}$ Binding to Immobilized Tropoelastin. Using proteomic analysis (www.iut-arles.up.univ-mrs.fr/w3bb/d_abim/compo-p.html), pH titration curves were calculated for FnBPA$_{37-544}$ and tropoelastin. FnBPA$_{37-544}$ binding to tropoelastin was then examined as described above using HBS−Ca buffer at different pH values ranging from 3 to 11. FnBPA$_{37-544}$ was injected at a concentration of 1000 nM in HBS−Ca over the surface of immobilized tropoelastin, and sensorgrams were obtained. The maximum binding R_{max} was plotted against pH.

Analysis of Data. Rate constants for association (k_a) and dissociation (k_d) and the equilibrium dissociation constant (K_D) were obtained by globally fitting the data using the BIAevaluation software version 3.0 using the simple 1:1 Langmuir binding model. This method was preferred as the equilibrium binding state was not reached. All experiments were performed in triplicate. Statistical analysis of the curve fitting at both dissociation and association phases of the sensorgrams showed χ^2 values of less than 3.5 for k_d and less than 10 for k_a.

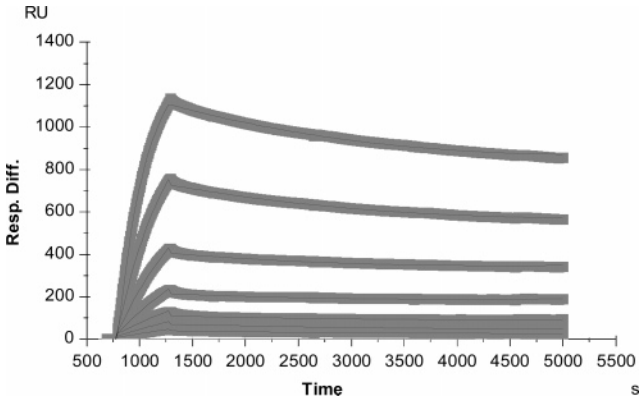

FIGURE 3: SPR analysis of rAFnBPA$_{37-544}$ binding full-length tropoelastin at pH 7.0. Tropoelastin was immobilized on the surface of a CM5 sensor chip. rAFnBPA$_{37-544}$ was passed over the surface at concentrations ranging from 500 to 7.8 nM. A strong interaction was observed between the proteins with nonsaturable binding. The average response of duplicate experiments (gray) and the fitted curve (black) are shown.

Circular Dichroism (CD) Spectroscopy. rAFnBPA$_{37-511}$ wild type, N304A, F306A, and N304A/F306A protein samples were dialyzed into 1 mM Tris-HCl, pH 7.4. Far-UV CD data were collected using a Jasco J-810 spectropolarimeter. Five scans were averaged for each spectrum, and the contribution from buffer was subtracted in each case. CD spectra were plotted over the 200−300 nm wavelength range and shown to be similar to that of the wild-type protein.

RESULTS

Binding of rAFnBPA$_{37-544}$ to Full-Length Tropoelastin. It has been reported previously that rAFnBPA$_{37-544}$ binds immobilized α-elastin peptides in a dose-dependent and saturable manner (*12*). We investigated if rAFnBPA$_{37-544}$ could bind to the elastin monomer, tropoelastin. Surface plasmon resonance (SPR) was carried out to measure binding of recombinant rAFnBPA proteins to immobilized human tropoelastin. A K_D of 29 ± 0.1 nM was obtained for rAFnBPA$_{37-544}$ binding to full-length tropoelastin (Figure 3). This is the first evidence that a staphylococcal cell wall anchored surface protein can bind the tropoelastin monomer.

Binding of rAFnBPA$_{37-544}$ to Tropoelastin Truncates. SPR was carried out to test the interaction of rAFnBPA$_{37-544}$ to three separate segments of tropoelastin, encompassing the N terminus of the protein to domain 18 (SHELN-18), domains 17−27 (SHEL17−27), and the region from domain 27 to the C terminus of the protein (SHEL27-C) (Figure 4). rAFnBPA$_{37-544}$ bound to all three segments of tropoelastin (Table 1). rAFnBPA$_{37-544}$ interacted with SHELN-18 with a dissociation constant of 31 ± 0.1 nM. A slightly weaker interaction was observed between rAFnBPA$_{37-544}$ and SHEL17−27 with a K_D of 57 ± 0.4 nM. rAFnBPA$_{37-544}$ interacted with SHEL27-C in a complex manner precluding confident kinetic data. It is clear that FnBPA is capable of binding all three parts of tropoelastin. This multiple site binding performance is similar to that seen for MAGP-1 (*18*) with tropoelastin and indicates that FnBPA binds sequence

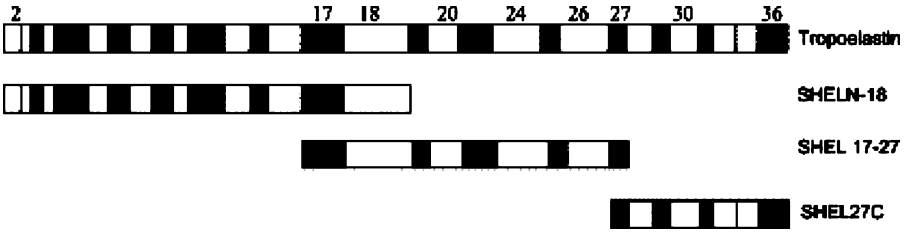

FIGURE 4: Domain structure of tropoelastin constructs. The domain structure of full-length human tropoelastin is compared with that of constructs SHELN-18, SHEL17−27, and SHEL27-C, spanning domains 2−18, 17−27, and 27−36, respectively. White segments represent hydrophobic domains while black segments represent hydrophilic domains.

Table 1: Binding of rAFnBPA$_{37-544}$ to Tropoelastin Constructs at pH 7[a]

construct	k_a [1/(M s)]	k_d (1/s)	K_D (nM)	χ^2
tropoelastin	$(7.10 \pm 0.02) \times 10^3$	$(2.00 \pm 0.002) \times 10^{-4}$	28 ± 0.1	4.7
SHELN-18	$(8.80 \pm 0.02) \times 10^3$	$(2.80 \pm 0.005) \times 10^{-4}$	31 ± 0.1	0.2
SHEL17−27	$(7.95 \pm 0.05) \times 10^3$	$(2.15 \pm 0.005) \times 10^{-3}$	270 ± 3	9.2

[a] The rate association constant (k_a), the rate dissociation constant (k_d), and the equilibrium dissociation constant (K_D) of rAFnBPA$_{37-544}$ binding to tropoelastin, SHELN-18, and SHEL17−27 were calculated by curve fitting using BiaEvaluation 4.1. The standard error (SE) and goodness of the fit (χ^2) are also given.

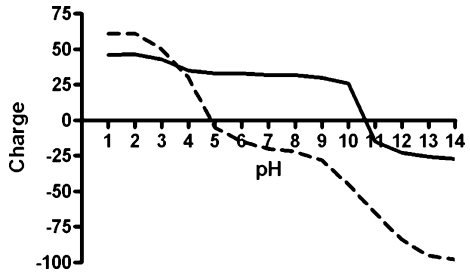

FIGURE 5: Titration curve for rAFnBPA$_{37-544}$ and tropoelastin. rAFnBPA$_{37-544}$ (broken line) undergoes a charge transition at its p*I* 5 and then becomes further negatively charged at pH >10. Tropoelastin undergoes a charge transition at its basic p*I* of 11 (solid line).

elements that are present in all three tropoelastin truncates. Tropoelastin contains numerous repeat sequences.

Effect of pH on the rAFnBPA−Tropoelastin Interaction. To investigate the FnBPA−tropoelastin interaction in more detail, SPR experiments were carried out using varying pH. Using proteomic analysis, titration curves of rAFnBPA$_{37-544}$ and tropoelastin were generated. Tropoelastin undergoes a sharp isoelectric transition at pH 11. This contrasts to rAFnBPA$_{37-544}$ which has an isoelectric point of 5 and remains only slightly negatively charged until pH above 10 (Figure 5). The effect of pH on the binding of these two proteins was investigated. When rAFnBPA$_{37-544}$ was injected over a tropoelastin-coated surface at various pHs, the response differed. At low pH the interaction was strong with nonsaturable binding. As the pH increased, the interaction weakened and saturable binding was observed at pH 10.6. By pH 11, under controlled conditions all interactions between the proteins had ceased (Figure 6).

Truncation of rAFnBPA$_{37-544}$ at the N and C Terminus. Following more detailed molecular analysis of FnBPA (*10*, *11*), it was noted that the recombinant protein used in experiments above (rAFnBPA$_{37-544}$) contained a fibronectin-binding motif at its C terminus. Indeed, this protein supported binding to immobilized fibronectin in solid-phase ELISA assays (data not shown). The true A domain was redefined to span residues 37−511. Recombinant protein rAFnBPA$_{37-511}$ was no longer able to bind fibronectin but retained the ability

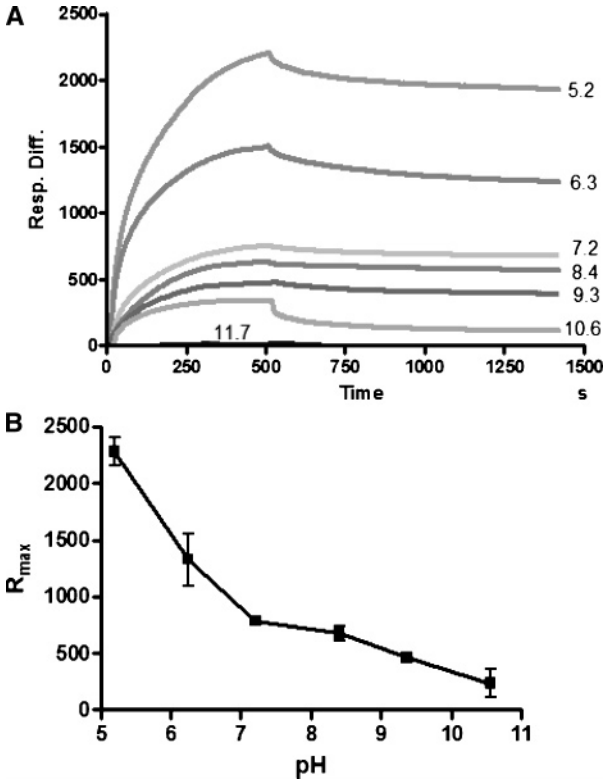

FIGURE 6: rAFnBPA$_{37-544}$ binding to tropoelastin over a pH range of 5.2−11.7. (A) rAFnBPA$_{37-544}$ bound strongly to tropoelastin at low pH with the interaction weakening at higher pH until no interaction was observed at pH 11.7. (B) A plot of maximum response vs pH highlights that the interaction is strongly dependent on pH.

to bind to immobilized fibrinogen and α-elastin. A further truncate, rAFnBPA$_{194-511}$, encompassing only subdomains N2 and N3 of region A was also able to bind to immobilized fibrinogen and α-elastin with similar affinity to that of rAFnBPA$_{37-511}$ (*13*). These two proteins were then tested for their ability to bind to immobilized tropoelastin by SPR analysis. Both proteins bound to tropoelastin in a dose-dependent manner with similar affinities. rAFnBPA$_{37-511}$ generated a dissociation constant of 127 ± 4 nM. A similar K_D of 146 ± 6 nM was calculated for the binding of

Table 2: Binding of rAFnBPA Constructs to Immobilized Tropoelastin[a]

protein	k_a [1/(Ms)]	SE k_a	χ^2 k_a	k_d (1/s)	SE k_d	χ^2 k_d	K_D (nM)	SE K_D
rAFnBPA$_{194-511}$	1.07e^4	452	9.49	1.47e^{-3}	5.91e^{-5}	3.49	146	6
rAFnBPA$_{37-511}$ wt	1.34e^4	672	9.74	1.42e^{-3}	4.63e^{-5}	1.98	127	4
rAFnBPA$_{37-511}$ R224A	9.74e^3	489	9.73	1.79e^{-3}	8.81e^{-5}	3.17	201	10
rAFnBPA$_{37-511}$ N304A	2.13e^4	1120	9.49	6.75e^{-4}	8.7e^{-5}	2.52	27	4
rAFnBPA$_{37-511}$ F306A	1.02e^4	457	9.64	1.29e^{-3}	6.58e^{-5}	2.36	135	7
rAFnBPA$_{37-511}$ L498A	9.53e^3	530	9.81	1.74e^{-3}	8.4e^{-5}	2.74	179	9
rAFnBPA$_{37-511}$ N304A/F306A	1.45e^4	319	9.76	2.5e^{-3}	1.32e^{-4}	1.65	171	9

[a] The rate association constant (k_a), the rate dissociation constant (k_d), and the equilibrium dissociation constant (K_D) of rAFnBPA constructs binding to full-length tropoelastin were calculated by curve fitting using BiaEvaluation 4.1. The standard error (SE) and goodness of the fit (χ^2) are also given.

rAFnBPA$_{194-511}$ (Table 2). This confirms previous data that the N1 subdomain of region A is not involved in ligand binding. These data show a 5-fold decrease in affinity for these constructs compared to rAFnBPA$_{37-544}$; however, all three proteins bind to tropoelastin in the low nanomolar range, which indicates a significant biological interaction.

Analysis of Site-Directed Mutants of rAFnBPA$_{37-511}$. Any further truncation of rAFnBPA$_{194-511}$ would likely impinge on the predicted structural fold of the protein so a site-specific approach was adopted. A theoretical model of the N23 subdomains of FnBPA was generated on the basis of the known crystal structure of ClfA (*14*). The segment of fibrinogen to which this protein binds was docked in silico into the putative ligand-binding trench situated between N2 and N3. This model was used to predict residues in FnBPA that may interact with a ligand. Several residues were targeted for alanine substitution, and the resulting recombinant proteins were tested for ligand binding. Some mutants had reduced affinity for fibrinogen and α-elastin with rAFnBPA$_{37-511}$ N304A, rAFnBPA$_{37-511}$ F306A, and a double mutant, rAFnBPA$_{37-511}$ N304A/F306A, all showing a dramatic loss in ligand binding (*13*). The position of residues N304 and F306 of rAFnBPA is indicated in Figure 2. The far-UV circular dichroism (CD) data of rAFnBPA$_{37-511}$ N304A and rAFnBPA$_{37-511}$ N304A/F306A were not detectably different from that of the wild-type rAFnBPA$_{37-511}$ protein (data not shown). The batch of rAFnBPA$_{37-511}$ F306A tested did show a slight alteration in spectrum in the 210−200 nm range. This protein, however, behaved as expected in unrelated assays, and the double mutant containing this F306A mutation was unaffected. We conclude that substitutions did not dramatically alter the conformation of the protein as further evidenced by the similar binding affinity for each purified variant protein to five monoclonal anti-rAFnBPA antibodies (data not shown).

Five alanine-substituted proteins of rAFnBPA$_{37-511}$ were tested for their ability to bind to immobilized tropoelastin by SPR. The proteins chosen contained substitutions which caused various levels of decreased affinity for α-elastin (L498A, R224A, and N304A) and those which showed undetectable binding to immobilized α-elastin by ELISA methods (F306A, N304A/F306A) (*13*). SPR analysis shows that these recombinant proteins bind to tropoelastin with the same affinity as rAFnBPA$_{37-511}$ (Table 2). Dissociation constants of 135 ± 7 and 171 ± 9 nM were obtained for proteins rAFnBPA$_{37-511}$ F306A and rAFnBPA$_{37-511}$ N304A/F306A, respectively. Two other substituted proteins, rAFnBPA$_{37-511}$ R224A and rAFnBPA$_{37-511}$ L498A, also showed no defect in tropoelastin binding, having K_Ds of 201 ± 10 and 179 ± 9 nM, respectively. The k_a values for these proteins range from 9.53 × 10^3 to 1.45 × 10^4 with k_d values ranging from 1.29 × 10^{-3} to 2.5 × 10^{-3}.

rAFnBPA$_{37-511}$ N304A had an ∼4.5-fold increased affinity for tropoelastin with a K_D of 27 ± 4 nM, which is similar to that seen for the initial rAFnBPA$_{37-544}$ protein to tropoelastin. This decreased dissociation constant is due to the contribution of both an increased k_a and a decreased k_d to the final K_D value for this protein. The errors associated with both k_a and k_d of this interaction are quite large. If this increased affinity is reproducible, a corresponding increased affinity should be seen for the double mutant rAFnBPA$_{37-511}$ N304A/F306A. However, this mutant does not have an increased affinity for tropoelastin. N304 is not essential to binding. We conclude that the amino acids located in the interior of the rAFnBPA protein, around the putative fibrinogen/α-elastin-binding trench between subdomains N2 and N3, are not involved in tropoelastin binding.

DISCUSSION

We demonstrated that FnBPA can directly bind tropoelastin. rAFnBPA$_{37-544}$ bound strongly to full-length tropoelastin with a K_D of 28 ± 0.1 nM. Binding to full-length tropoelastin was identical to that seen between rAFnBPA$_{37-544}$ and SHELN-18 with almost identical k_a and k_d and subsequent K_D values, but there was weaker binding to SHEL17−27. C-Terminal SHEL27-C showed strong binding to rAFnBPA$_{37-544}$ with a slow complex dissociation that precluded curve fitting to standard kinetic models. We conclude that FnBPA interacts with tropoelastin at multiple sites and may do so by interacting with common repetitive sequence elements. It is possible that smaller tropoelastin fragments may help to identify binding motifs for FnBPA, but this approach has not proved productive for other proteins that bind multiple sites in tropoelastin (*18*) probably because of the complex use of varied repeats-in-repeats in tropoelastin, the loss of secondary structure, and the likelihood of cooperative interactions that facilitate the binding affinities presented here.

The interaction between rAFnBPA$_{37-544}$ and tropoelastin was monitored at varying pHs with the aim of determining the nature of the interaction. At less than pH 11 an interaction was observed between the two proteins. At pH 11 and above no binding occurred, highlighting the pH-dependent nature of the interaction. At pH 11 or above, it is possible that the loss of binding is due to conformational changes induced by such a basic environment but was not due to a simple regeneration of the sensor chip surface (data not shown). The FnBPA−tropoelastin interaction withstands a broad

range of pH, and the sensorgram obtained at pH 10.6 persistently demonstrates a specific dose-dependent interaction. Titratable positively charged lysines on the surface of tropoelastin may contribute to the interaction. Indeed, at pH >5, rAFnBPA$_{37-544}$ is negatively charged and is drawn to interact with the positively charged lysines of tropoelastin. We propose that ionic interactions between positive regions on tropoelastin and negatively charged regions of rAFnBPA$_{37-544}$ stabilize the binding between the proteins. These multiple surface−surface interactions promote dose-dependent binding in SPR analysis and could indicate a mechanism to allow *S. aureus* to bind to human tropoelastin in vivo.

Subsequent to the mapping of the 11 fibronectin-binding motifs of FnBPA by other researchers (*10*), it was noted that the recombinant rAFnBPA protein used in the above assays (rAFnBPA$_{37-544}$) contained a fibronectin-binding motif at its C terminus. A protein lacking this motif, rAFnBPA$_{37-511}$, was previously shown to be defective in fibronectin binding but retained fibrinogen and α-elastin binding ability (*13*). We have shown here that this protein can also bind immobilized tropoelastin in a dose-dependent manner, generating a K_D of 127 ± 4 nM. This represents a 4.5-fold decrease in affinity compared to that of rAFnBPA$_{37-544}$, which can be explained by the loss of surface−surface interactions occurring between the negatively charged 512−544 sequence and the positive lysines of tropoelastin. A further truncate of rAFnBPA lacking the N1 subdomain, rAFnBPA$_{194-511}$, had an affinity comparable to rAFnBPA$_{37-511}$ for tropoelastin, supporting previous results showing that this FnBPA subdomain has no role in ligand binding.

The investigation of the binding of rAFnBPA to other ligands highlighted crucial residues buried within the FnBPA molecule along the putative fibrinogen-binding trench. Recombinant rAFnBPA$_{37-511}$ proteins with specific alanine substitutions were tested for binding to tropoelastin. The range of K_Ds observed for the alanine-substituted rAFnBPA$_{37-511}$ proteins, however, did not differ significantly from that of wt rAFnBPA$_{37-511}$. However, rAFnBPA$_{37-511}$ N304A had an ∼5-fold decrease in K_D, bringing it into the affinity range seen for that of the initial rAFnBPA$_{37-544}$ construct. This shows that residues located along the interior hydrophobic trench situated between N2 and N3 of region A of FnBPA are not involved in tropoelastin binding. This supports the hypothesis that FnBPA binds to tropoelastin by a distinct mechanism.

This is the first demonstration that the A domain of FnBPA from *S. aureus* promotes binding to tropoelastin. The binding of *S. aureus* surface proteins to multiple ligands is widely recognized. FnBPA is indeed a multifunctional protein, binding diverse matrix proteins such as fibronectin, fibrinogen, elastin, and now tropoelastin.

S. aureus encounters elastin on its journey through elastin-rich artery walls, traversing the extracellular space beneath the basement membrane of endothelial cells in tissue such as the elastin-containing lung and around the synovial lining of various joints. The interaction of *S. aureus* with the surface of tropoelastin-secreting endothelial cells has been known for some time (*20*, *21*). *S. aureus* interacts with integrins on the surfaces of other elastin synthesizing cells including elastogenic fibroblasts through bridging molecules such as fibronectin (*22*). This interaction ultimately results in the internalization of *S. aureus* by such endothelial or fibroblast cells and is likely to interfere with elastogenesis (*23*). Recent studies have also demonstrated the important contribution of FnBPA to the adherence of *S. aureus* to intact endothelium in vivo (*24*). The close proximity of this bacterium to the surface of these host cells provides multiple opportunities to interact with the tropoelastin monomer on the cell surface. Tropoelastin synthesis in fibroblast and endothelial cells is highest in fetal and infant development. *S. aureus* is a known pathogen of low birth weight neonates, causing skin and other tissue infections and often causing systemic sepsis. The high mortality of such infections has led to clinical trials testing the efficacy of antistaphylococcal IgG-based prophylactics (*25*), and it is possible that *S. aureus* interactions with secreted tropoelastin on these cells aid in establishing infection and inhibiting ECM repair.

During the course of an infection, bacterial and host elastases are both active. *S. aureus* produces a cysteine protease ScpB which degrades elastin tissue and is inhibited by α2-macroglobulin (*26*). It also produces a serine protease, SspA, which inactivates alpha-1-proteinase inhibitor (alpha 1PI), a major factor which protects lungs from phagocytic proteases (*27*). A staphylococcal zinc metalloprotease, lysostaphin, also has elastolytic activity (*28*) as does Ecp, a homologue of ScpB, found in *Staphylococcus epidermidis* (*29*). In addition to its own repertoire of elastin-degrading enzymes, *S. aureus* has been shown to induce the production of host matrix proteinases in human dermal and synovial fibroblasts (*30*). As the bacterium traverses the extracellular matrix during systemic infection, it will therefore encounter varying states of elastin tissue, in the process of being degraded or subsequently repaired. Two elastin repair processes have been described, namely, salvage (*31*) and de novo synthesis (*32*) methods. The latter involves increased tropoelastin synthesis and secretion from cells in elastin-damaged tissue. These degradation and repair processes result in the exposure of a heterogeneous mix of elastin peptides and tropoelastin monomers, all of which *S. aureus* is capable of binding via FnBPA. The extraordinary adaptability of FnBPA may help to explain the persistent nature of elastin-specific *S. aureus* infections.

ACKNOWLEDGMENT

We thank Orsola Regalia for the production of recombinant tropoelastin and tropoelastin truncates.

REFERENCES

1. Williams, R. E. (1963) Healthy carriage of *Staphylococcus aureus*: its prevalence and importance, *Bacteriol. Rev. 27*, 56−71.
2. Fowler, V. G., Jr., Miro, J. M., Hoen, B., Cabell, C. H., Abrutyn, E., Rubinstein, E., Corey, G. R., Spelman, D., Bradley, S. F., Barsic, B., Pappas, P. A., Anstrom, K. J., Wray, D., Fortes, C. Q., Anguera, I., Athan, E., Jones, P., van der Meer, J. T., Elliott, T. S., Levine, D. P., and Bayer, A. S. (2005) *Staphylococcus aureus* endocarditis: a consequence of medical progress, *J. Am. Med. Assoc. 293*, 3012−3021.
3. McDevitt, D., Francois, P., Vaudaux, P., and Foster, T. J. (1994) Molecular characterization of the clumping factor (fibrinogen receptor) of *Staphylococcus aureus*, *Mol. Microbiol. 11*, 237−248.
4. Ni Eidhin, D., Perkins, S., Francois, P., Vaudaux, P., Hook, M., and Foster, T. J. (1998) Clumping factor B (ClfB), a new surface-located fibrinogen-binding adhesin of *Staphylococcus aureus*, *Mol. Microbiol. 30*, 245−257.

5. Wann, E. R., Gurusiddappa, S., and Hook, M. (2000) The fibronectin-binding MSCRAMM FnbpA of *Staphylococcus aureus* is a bifunctional protein that also binds to fibrinogen, *J. Biol. Chem. 275*, 13863−13871.
6. Signas, C., Raucci, G., Jonsson, K., Lindgren, P. E., Anantharamaiah, G. M., Hook, M., and Lindberg, M. (1989) Nucleotide sequence of the gene for a fibronectin-binding protein from *Staphylococcus aureus*: use of this peptide sequence in the synthesis of biologically active peptides, *Proc. Natl. Acad. Sci. U.S.A. 86*, 699−703.
7. Jonsson, K., Signas, C., Muller, H. P., and Lindberg, M. (1991) Two different genes encode fibronectin binding proteins in *Staphylococcus aureus*. The complete nucleotide sequence and characterization of the second gene, *Eur. J. Biochem. 202*, 1041−1048.
8. Speziale, P., Raucci, G., Visai, L., Switalski, L. M., Timpl, R., and Hook, M. (1986) Binding of collagen to *Staphylococcus aureus* Cowan 1, *J. Bacteriol. 167*, 77−81.
9. Walsh, E. J., O'Brien, L. M., Liang, X., Hook, M., and Foster, T. J. (2004) Clumping factor B, a fibrinogen-binding MSCRAMM (microbial surface components recognizing adhesive matrix molecules) adhesin of *Staphylococcus aureus*, also binds to the tail region of type I cytokeratin 10, *J. Biol. Chem. 279*, 50691−50699.
10. Schwarz-Linek, U., Werner, J. M., Pickford, A. R., Gurusiddappa, S., Kim, J. H., Pilka, E. S., Briggs, J. A., Gough, T. S., Hook, M., Campbell, I. D., and Potts, J. R. (2003) Pathogenic bacteria attach to human fibronectin through a tandem beta-zipper, *Nature 423*, 177−181.
11. Pilka, E. S., Werner, J. M., Schwarz-Linek, U., Pickford, A. R., Meenan, N. A., Campbell, I. D., and Potts, J. R. (2006) Structural insight into binding of *Staphylococcus aureus* to human fibronectin, *FEBS Lett. 580*, 273−277.
12. Roche, F. M., Downer, R., Keane, F., Speziale, P., Park, P. W., and Foster, T. J. (2004) The N-terminal A domain of fibronectin-binding proteins A and B promotes adhesion of *Staphylococcus aureus* to elastin, *J. Biol. Chem. 279*, 38433−38440.
13. Keane, F. M., Loughman, A., Valtulina, V., Brennan, M., Speziale, P., and Foster, T. J. (2007) Fibrinogen and elastin bind to the same region within the A domain of fibronectin binding protein A, an MSCRAMM of *Staphylococcus aureus*, *Mol. Microbiol. 63*, 711−723.
14. Deivanayagam, C. C., Wann, E. R., Chen, W., Carson, M., Rajashankar, K. R., Hook, M., and Narayana, S. V. (2002) A novel variant of the immunoglobulin fold in surface adhesins of *Staphylococcus aureus*: crystal structure of the fibrinogen-binding MSCRAMM, clumping factor A, *EMBO J. 21*, 6660−6672.
15. Rosenbloom, J. (1982) Elastin: biosynthesis, structure, degradation and role in disease processes, *Connect. Tissue Res. 10*, 73−91.
16. Cox, B. A., Starcher, B. C., and Urry, D. W. (1973) Coacervation of alpha-elastin results in fiber formation, *Biochim. Biophys. Acta 317*, 209−213.
17. Clarke, A. W., Wise, S. G., Cain, S. A., Kielty, C. M., and Weiss, A. S. (2005) Coacervation is promoted by molecular interactions between the PF2 segment of fibrillin-1 and the domain 4 region of tropoelastin, *Biochemistry 44*, 10271−10281.
18. Clarke, A. W., and Weiss, A. S. (2004) Microfibril-associated glycoprotein-1 binding to tropoelastin: multiple binding sites and the role of divalent cations, *Eur. J. Biochem. 271*, 3085−3090.
19. Rodgers, U. R., and Weiss, A. S. (2004) Integrin alpha v beta 3 binds a unique non-RGD site near the C-terminus of human tropoelastin, *Biochimie 86*, 173−178.
20. Tompkins, D. C., Hatcher, V. B., Patel, D., Orr, G. A., Higgins, L. L., and Lowy, F. D. (1990) A human endothelial cell membrane protein that binds *Staphylococcus aureus* in vitro, *J. Clin. Invest. 85*, 1248−1254.
21. Tompkins, D. C., Blackwell, L. J., Hatcher, V. B., Elliott, D. A., O'Hagan-Sotsky, C., and Lowy, F. D. (1992) *Staphylococcus aureus* proteins that bind to human endothelial cells, *Infect. Immun. 60*, 965−969.
22. Sinha, B., Francois, P. P., Nusse, O., Foti, M., Hartford, O. M., Vaudaux, P., Foster, T. J., Lew, D. P., Herrmann, M., and Krause, K. H. (1999) Fibronectin-binding protein acts as *Staphylococcus aureus* invasin via fibronectin bridging to integrin alpha5beta1, *Cell. Microbiol. 1*, 101−117.
23. Schroder, A., Schroder, B., Roppenser, B., Linder, S., Sinha, B., Fassler, R., and Aepfelbacher, M. (2006) *Staphylococcus aureus* fibronectin binding protein-A induces motile attachment sites and complex actin remodeling in living endothelial cells, *Mol. Biol. Cell 17*, 5198−5210.
24. Kerdudou, S., Laschke, M. W., Sinha, B., Preissner, K. T., Menger, M. D., and Herrmann, M. (2006) Fibronectin binding proteins contribute to the adherence of *Staphylococcus aureus* to intact endothelium in vivo, *Thromb. Haemostasis 96*, 183−189.
25. Bloom, B., Schelonka, R., Kueser, T., Walker, W., Jung, E., Kaufman, D., Kesler, K., Roberson, D., Patti, J., and Hetherington, S. (2005) Multicenter study to assess safety and efficacy of INH-A21, a donor-selected human staphylococcal immunoglobulin, for prevention of nosocomial infections in very low birth weight infants, *Pediatr. Infect. Dis. J. 24*, 858−866.
26. Potempa, J., Dubin, A., Korzus, G., and Travis, J. (1988) Degradation of elastin by a cysteine proteinase from *Staphylococcus aureus*, *J. Biol. Chem. 263*, 2664−2667.
27. Nowak, D., and Miedzobrodzki, J. (1991) Serine proteinase from *Staphylococcus aureus* enhances elastin degradation by elastases in the presence of human alpha-1-proteinase inhibitor, *Antonie Van Leeuwenhoek 59*, 109−114.
28. Park, P. W., Senior, R. M., Griffin, G. L., Broekelmann, T. J., Mudd, M. S., and Mecham, R. P. (1995) Binding and degradation of elastin by the staphylolytic enzyme lysostaphin, *Int. J. Biochem. Cell Biol. 27*, 139−146.
29. Oleksy, A., Golonka, E., Banbula, A., Szmyd, G., Moon, J., Kubica, M., Greenbaum, D., Bogyo, M., Foster, T. J., Travis, J., and Potempa, J. (2004) Growth phase-dependent production of a cell wall-associated elastinolytic cysteine proteinase by *Staphylococcus epidermidis*, *Biol. Chem. 385*, 525−535.
30. Kanangat, S., Postlethwaite, A., Hasty, K., Kang, A., Smeltzer, M., Appling, W., and Schaberg, D. (2006) Induction of multiple matrix metalloproteinases in human dermal and synovial fibroblasts by *Staphylococcus aureus*: implications in the pathogenesis of septic arthritis and other soft tissue infections, *Arthritis Res. Ther. 8*, R176.
31. Stone, P. J., Morris, S. M., Martin, B. M., McMahon, M. P., Faris, B., and Franzblau, C. (1988) Repair of protease-damaged elastin in neonatal rat aortic smooth muscle cell cultures, *J. Clin. Invest. 82*, 1644−1654.
32. Foster, J. A., Rich, C. B., and Miller, M. F. (1990) Pulmonary fibroblasts: an in vitro model of emphysema. Regulation of elastin gene expression, *J. Biol. Chem. 265*, 15544−15549.

BI700454X